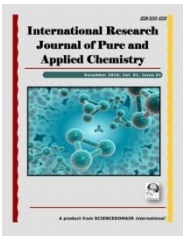

International Research Journal of Pure & Applied Chemistry
4(6): 762-772, 2014

SCIENCEDOMAIN *international*
www.sciencedomain.org

Matrix Isolation and Theoretical Study on the Photolysis of $CH_2ClCOCl$

Nobuaki Tanaka[1*] and Mayuko Nakata[1]

[1]Department of Environmental Science and Technology, Faculty of Engineering, Shinshu University, 4-17-1 Wakasato, Nagano 380-8553, Japan.

Authors' contributions

This work was carried out in collaboration between both authors. Author NT performed the experimental and computational studies, wrote the protocol and wrote the first draft of the manuscript. Author MN performed the experimental study. Both authors read and approved the final manuscript.

Original Research Article

Received 13th June 2014
Accepted 8th July 2014
Published 15th July 2014

ABSTRACT

UV light photolysis of chloroacetyl chloride ($CH_2ClCOCl$) has been investigated using infrared spectroscopy in cryogenic Ar, Kr, Xe and O_2 matrices. In all matrices, CHCl=C=O, HCl, CH_2Cl_2 and CO were produced, with the relative yields depending on the used matrix gas. The relative yield of CH_2Cl_2 formation to CHCl=C=O formation was greatly enhanced in Xe because of the external heavy atom effect, indicative of the formation of CH_2Cl_2 via the C–C or C–Cl bond cleavage in the triplet state. In $CH_2ClCOCl$/Ar, photoisomerization from *anti*- to *gauche*-$CH_2ClCOCl$ was also observed at the early stage of the irradiation. The results show that in Ar, the reactions predominantly proceed through concerted mechanisms.

Keywords: Chloroacetyl chloride; photolysis; cryogenic matrix; Ketene.

1. INTRODUCTION

Chlorinated acetyl chlorides are produced through the oxidation of chlorinated ethenes [1,2]. The photodissociation of chlorinated acetyl chlorides is an environmentally important

**Corresponding author: Email: ntanaka@shinshu-u.ac.jp;*

process. The potential release of Cl by photochemical reaction in the atmosphere enhances the Cl cycle in ozone depletion. In the oxidation of chlorinated ethenes initiated by Cl, relatively high yields of chlorinated acetyl chloride were reported by Hasson and Smith [3]. In Ar matrix, hydroxyl radical reacts with tetrachloroethene to yield trichloroacetyl chloride [4].

Chloroacetyl chloride can exist as an *anti* or *gauche* conformer depending on the difference in the relative orientation of the two C–Cl bonds [5]. Infrared (IR) spectra of chloroacetyl chloride in gas, liquid and solid phases, and matrix-isolated were measured by many groups [6-10]. Allen and Russell studied the pyrolysis of chloroacetyl chloride using IR laser, in which 1,2-HCl elimination occurred to produce chloroketene [11]. In Xe matrix, Davidovics et al. obtained the photolysis product of chloroketene [12]. Previously, we studied the photolysis of CCl_3COCl in Ar and O_2 matrices, in which C–C bond cleavage was found to be the major reaction path [13]. In contrast, acetyl chloride (CH_3COCl) underwent the four-center elimination to yield the HCl·ketene complex in the S_0 state after internal conversion from the S_1 state [14,15]. For the photolysis of CF_3COCl, CF_3Cl and CO were produced via the radical mechanism [16]. The fact that the substitution of a halogen atom could change the reaction mechanism is of great interest.

In the present study, we investigated the UV light photolysis of $CH_2ClCOCl$ in cryogenic Ar, Kr, Xe and O_2 matrices with the aid of theoretical calculations using the B3LYP and MP2 methods. The computational results were used to interpret the IR spectra. Moreover, the reaction mechanism was discussed on the basis of the differences observed in the four matrices.

2. EXPERIMENTAL DETAILS

Light irradiation was performed using a low-pressure mercury short arc lamp (HAMAMATSU L937-04, $\lambda > 253.7$ nm). IR spectra were measured in the range of 4000–700 cm^{-1} with a resolution of 1.0 cm^{-1} using a Fourier transform IR spectrometer (SHIMADZU 8300A) coupled with a liquid-nitrogen-cooled MCT detector. Each spectrum was obtained by acquiring 128 scans. A closed-cycle helium cryostat (Iwatani M310/CW303) was used to control the temperature of the matrix.

Argon (Nippon Sanso, 99.9999%), krypton (Taiyo Sanso), xenon (Nippon Sanso) and O_2 (Okaya Sanso) were used without further purification. Chloroacetyl chloride (Wako Pure Chemicals) was used after freeze–pump–thaw cycle at 77 K. Dichloromethane (Wako Pure Chemicals) was used as an authentic sample for product identification. The sample was diluted with the matrix gas to approximately 1/1000 (0.2 Torr sample and 200 Torr matrix gas) and was deposited on a CsI window at 6 K.

For product identification and energetic consideration, molecular orbital calculation was performed. Geometry optimizations were performed using the second-order Møller–Plesset theory (MP2) with the 6-311++G(3df,3pd) basis set and using the Becke's three-parameter hybrid density functional [17] in combination with the Lee–Yang–Parr correlation functional (B3LYP) [18] with the aug-cc-pV(T+d)Z basis set. Harmonic vibrational frequency calculation was performed to confirm the predicted structures as local minima and to elucidate the zero-point vibrational energy corrections. The vertical transition energy was calculated at the SAC-CI/D95+(d,p) level based on the structures optimized at the CCSD/D95+(d,p) level. All calculations were performed using Gaussian 09 [19].

3. RESULTS AND DISCUSSION

3.1 $CH_2ClCOCl$/Ar

A mixture of $CH_2ClCOCl$/Ar was deposited on a CsI window with a ratio of $CH_2ClCOCl$/Ar = 1/1000. In the IR spectrum obtained after deposition, a strong band was observed at 1829 cm^{-1}, which was attributed to the C=O stretching vibration of the *anti*-$CH_2ClCOCl$ [6,9]. Fig. 1(a) shows the IR difference spectrum obtained after irradiation at a wavelength >253.7 nm of the $CH_2ClCOCl$/Ar matrix for 210 min. The positive and negative bands indicate the growth and depletion, respectively, during the irradiation period. Table 1 lists the observed wavenumbers of the growth bands. Although the band at 1790 cm^{-1}, which was previously assigned to the C=O stretching vibration of *gauche*-$CH_2ClCOCl$, decreased concomitantly with the increase of the shoulder at 1784 cm^{-1}, the growth bands at 1140, 1060, 1054, 822, 813 and 810 cm^{-1} are in good agreement with those of *gauche*-$CH_2ClCOCl$ [9]. Based on far-IR spectrum measurements, Durig et al. determined that the enthalpy difference between the two rotamers was 587 cm^{-1} [6], at which the *anti* rotamer was more stable. The calculation at the B3LYP/aug-cc-pV(T+d)Z level indicated that the *anti* rotamer is more stable than the *gauche* rotamer by 599 cm^{-1} ($\Delta G°$ at 298 K), indicating that the *gauche*/*anti* population ratio before UV irradiation is 0.086/1 at 298 K. However, the population ratio was estimated to be 0.17 using the relative integrated absorbance ratio (I_{1790}/I_{1829}) of 0.20 and the calculated IR intensity ratio of 1.15 at the B3LYP/aug-cc-pV(T+d)Z level, which is larger than that expected from the Boltzmann distribution. The frequency calculation with the anharmonic correction at the MP2/6-311++G(3df,3pd) level revealed that the band at 1790 cm^{-1} was assigned to the overtone band of the CH_2 rocking vibration of *anti*-$CH_2ClCOCl$. The barrier height for the conversion from the *anti* to *gauche* rotamer was calculated to be 1098 cm^{-1} in the S_0 ground state, indicating that the conversion is not expected to occur at 7 K in the absence of UV irradiation. UV irradiation yielded an increase in the population of the less stable rotamer. Further irradiation enabled to distinguish the product bands due to different growth behaviors. Fig. 1(b) shows the IR difference spectrum obtained by subtracting the spectrum measured after 210 min irradiation from that measured after 630 min irradiation. In addition to the *anti*-$CH_2ClCOCl$ depletion, the bands due to *gauche*-$CH_2ClCOCl$ decreased. The band at 1784 cm^{-1}, which shows depletion in Fig. 1(b), was much broader than that in Fig. 1(a), which enabled us to reconfirm that the band at 1784 cm^{-1} corresponded to the C=O stretching vibration band of *gauche*-$CH_2ClCOCl$ overlapping with the band due to *anti*-$CH_2ClCOCl$. Prominent doublet bands at 2153 and 2147 cm^{-1} continued to grow at different growth rates during the prolonged irradiation period. Three doublet bands at 1302 and 1297 cm^{-1}, 1120 and 1113 cm^{-1}, and 808 and 804 cm^{-1} showed the same growth behavior as those of the 2153 and 2147 cm^{-1} bands which were assigned to the C=C stretching, C–H in-plane bending, C–Cl stretching and C=O stretching vibrations of CHCl=C=O, respectively. Davidovics et al. measured the IR bands of CHCl=C=O at 2141.4, 1293, 1107 and 842.2 cm^{-1} in Xe matrix [12]. The bands at 2857 and 2809 cm^{-1} were assigned to the stretching vibration of HCl and their growth behaviors corresponded to those of the bands at 2147 and 2153 cm^{-1} of CHCl=C=O, respectively. The weak bands at 1268 and 749 cm^{-1} were assigned to the CH_2 wagging and CCl_2 antisymmetric stretching vibrations of CH_2Cl_2, respectively, by comparing with the wavenumbers of authentic CH_2Cl_2 in Ar. Moreover, the weak bands in the 3000–2700 cm^{-1} region, except those of HCl were determined as the combination and overtone bands. In contrast to the photolysis of CCl_3COCl, the band due to COCl was not observed.

Table 1. FTIR spectra of photochemical reaction products of the $CH_2ClCOCl$ in the Ar, Kr, Xe and O_2 matrices

Wavenumber/cm^{-1}				species
Ar	**Kr**	**Xe**	**O_2**	
3134			3132	CHCl=C=O···HCl π complex
3115			3115	CHCl=C=O···HCl n complex
2885				HCl
2857	2843	2826	2850	HCl···CHCl=C=O n complex
2816/2809	2810/2804	2808	2805	HCl···CHCl=C=O π complex
	2762			$CHCl_2^-$ [20]
			2343	$^{12}CO_2$
			2276	$^{13}CO_2$
2153	2149	2146	2157	CHCl=C=O···HCl π complex
2147	2145	2142	2152	CHCl=C=O···HCl n complex
2140	2142	2133	2145	CO
			2107	O_3 v_1 +v_3 [21]
2101				^{13}CO
2090	2097			CHCl=C=O
			2037	CO_3
1784				*gauche*-$CH_2ClCOCl$ overlapped with combination band of *anti*-$CH_2ClCOCl$
1302	1303	1293		CHCl=C=O···HCl π complex
1297				CHCl=C=O···HCl n complex
1268	1267	1263	1268	CH_2Cl_2
1140			1136	*gauche*-$CH_2ClCOCl$
1120				CHCl=C=O···HCl π complex
1113		1112	1112	CHCl=C=O···HCl n complex
1109				CHCl=C=O···HCl n complex
			1101	O_3 v_1 [22]
1060				*gauche*-$CH_2ClCOCl$
1054			1057	*gauche*-$CH_2ClCOCl$
			1036	O_3 v_3 [22]
		954		Xe_2H^+ [23]
		900		$CHCl_2$ [24]
		892		$CHCl_2$ [24]
	853			Kr_2H^+ [23]
		844		Xe_2H^+ [23]
822			820	*gauche*-$CH_2ClCOCl$
818			816	*gauche*-$CH_2ClCOCl$
813				*gauche*-$CH_2ClCOCl$
810			810	*gauche*-$CH_2ClCOCl$
808			807	CHCl=C=O···HCl π complex
804			803	CHCl=C=O···HCl n complex
748	747	746	750	CH_2Cl_2
		731		Xe_2H^+ [23]

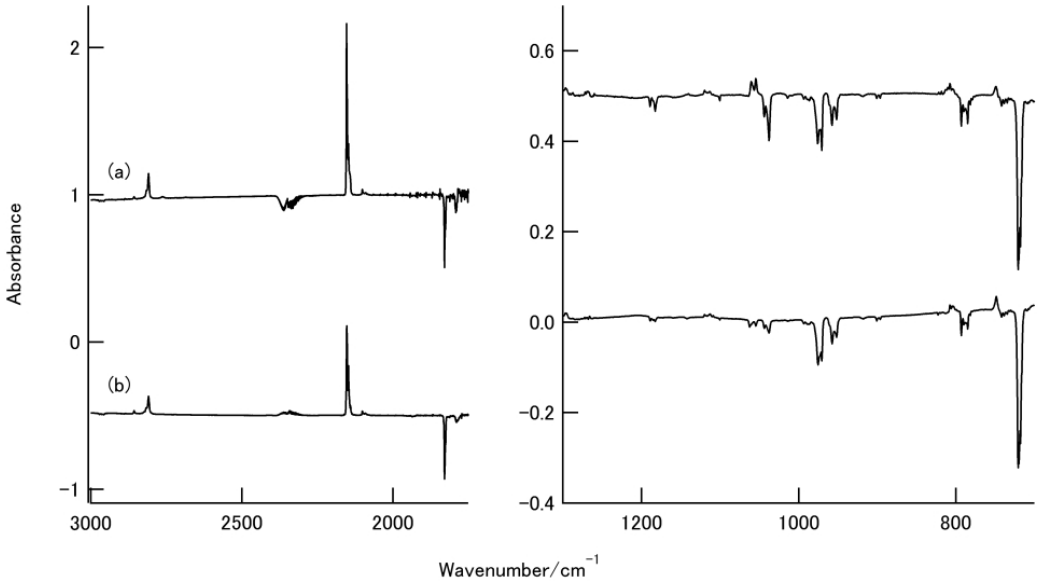

Fig. 1. Infrared difference spectra upon λ > 253.7 nm irradiation of the matrix $CH_2ClCOCl$/Ar = 1/1000. (a) 210−0 min and (b) 630−210 min

Two sets of bands assigned to CHCl=C=O vibrations were measured. They showed different growth behavior accompanying with the bands due to HCl different in wavenumbers, indicating the presence of two different structures of the CHCl=C=O···HCl complex in spite of the matrix site effect. As shown in Fig. 2, two stable structures were calculated for the CHCl=C=O···HCl complexesin which the hydrogen atom of HCl points to the carbon atom of CHCl (π complex) or O atom (n complex). Similar structures were proposed for the CH_2=C=O···HCl complexes [25]. Characteristic HCl stretching and C=O stretching vibrations for the two CHCl=C=O···HCl were calculated to be 2821 and 2177 cm^{-1}, respectively, for the π complex, and 2919 and 2172 cm^{-1}, respectively, for the n complex at the MP2/6-311++G(3df,3pd) level with anharmonic correction. Two species characterized by the absorption bands at 3134, 2809, 2153, 1302, 1120 and 808 cm^{-1}, and 3115, 2857, 2147, 1297, 1113 and 804 cm^{-1} were identified with the π and n complexes of CHCl=C=O···HCl, respectively.

3.2 $CH_2ClCOCl$/Kr and $CH_2ClCOCl$/Xe

Figs. 3(a) and 4(a) show the IR difference spectra obtained upon irradiation of the matrices $CH_2ClCOCl$/Kr and $CH_2ClCOCl$/Xe, respectively, at a wavelength >253.7 nm. The strong absorption bands observed at approximately 2145 cm^{-1} were assigned to the CO stretching vibrations of CHCl=C=O and CO. Due to the weak intensities of the bands of CHCl=C=O, except for the C=O stretching band, the presence of the two complexes was not evident, although splittings were observed in the 2145 cm^{-1} region. As observed in Figs. 2(b) and 3(b), the intensity of the higher wavenumber side of these bands decreased. The product CHCl=C=O was further photodissociated in the Kr and Xe matrices. SAC-CI calculation showed that the S_1 state of CHCl=C=O possesses the mixing characters of $\pi\sigma^*_{C-Cl}$ and πRydberg, –0.59 (HOMO → LUMO) – 0.53 (HOMO → LUMO + 1) + 0.48 (HOMO → LUMO + 3). Thus, the C–Cl bond dissociation would occur. Absorption bands due to CH_2Cl_2 were

observed at 1267 and 747 cm^{-1}, and 1263 and 746 cm^{-1}, in the Kr and Xe matrices, respectively. The band at 853 cm^{-1} in the Kr matrix was assigned to the v_3 of Kr_2H^+ [23]. The bands at 954, 844 and 731 cm^{-1} in the Xe matrix were assigned to the $v_3 + 2v_1$, $v_3 + v_1$ and v_3 of Xe_2H^+, respectively [23]. For comparison, the IR difference spectrum of the photolysis products of the matrix CH_2Cl_2/Xe is shown in Fig. 4(c). Similar product bands were observed at 954, 844 and 731 cm^{-1}, indicating that the photolysis product CH_2Cl_2 of $CH_2ClCOCl$ was also further decomposed to yield Kr_2H^+ or Xe_2H^+. Therefore, it is plausible that the band at 844 cm^{-1} which was previously assigned to the v_5 of CHCl=C=O, is reassigned to the $v_3 + v_1$ of Xe_2H^+.

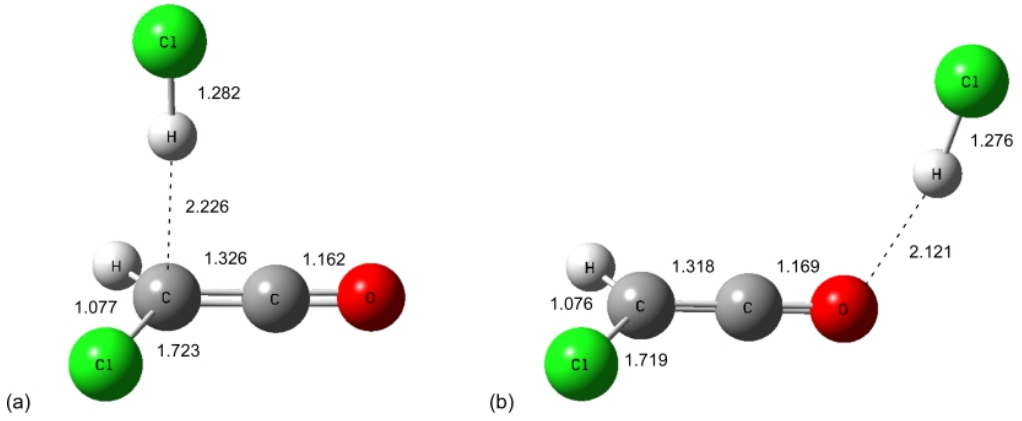

Fig. 2. Optimized equilibrium structures of the CHCl=C=O···HCl complexes calculated at the MP2/6-311++G(3df,3pd) level. Bond lengths are in Å. (a) π complex and (b) n complex

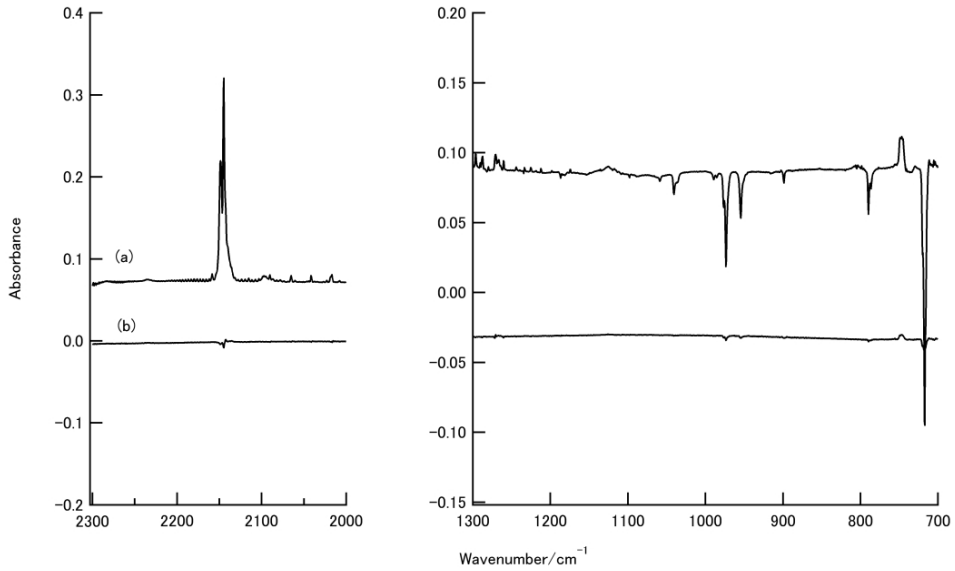

Fig. 3. Infrared difference spectra upon λ > 253.7 nm irradiation of the matrix $CH_2ClCOCl$/Kr = 1/1000 for 360 min. (a) 330−0 min and (b) 360−330 min

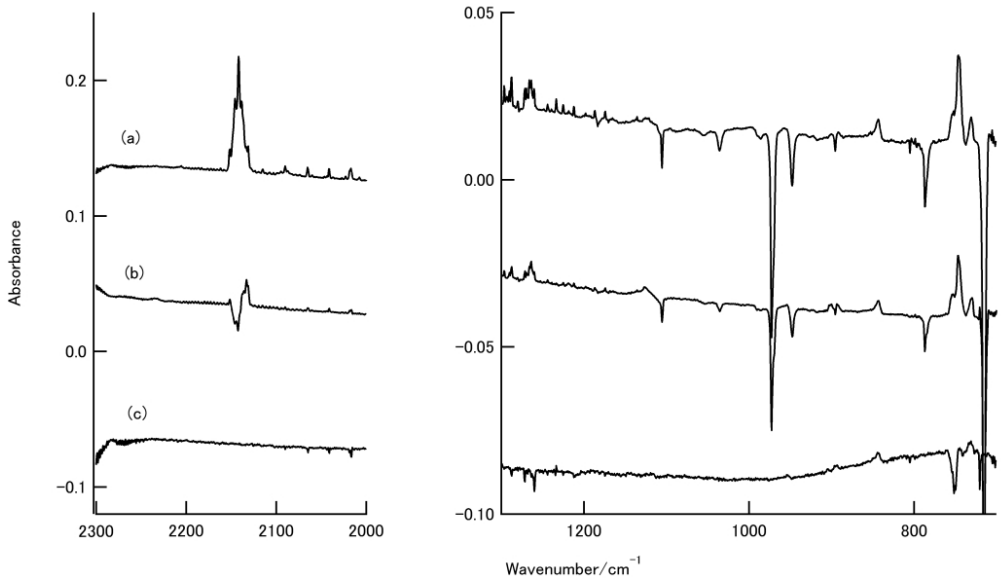

Fig. 4. Infrared difference spectra upon λ > 253.7 nm irradiation of the matrix $CH_2ClCOCl/Xe$ = 1/1000. (a) 180−0 min and (b) 420−180 min. (c) Infrared difference spectra upon λ > 253.7 nm irradiation for 180 min of the matrix CH_2Cl_2/Xe = 1/1000

3.3 $CH_2ClCOCl/O_2$

To clarify the route of CHCl=C=O and CH_2Cl_2 formation, i.e., radical or concerted mechanism, the reactive O_2 matrix was used. Fig. 5 shows the IR difference spectrum obtained after 300 min of the irradiation of the $CH_2ClCOCl/O_2$ matrix. Product bands were assigned by comparison with the spectrum observed in the photolysis of the CCl_3COCl/O_2 matrix [13]. Due to the fact that the photolysis occurred in O_2 at 253.7 nm, the band of ozone was prominent at 1038 cm^{-1} (v_3) [22]. Other O_3 absorption bands were observed at 2107 (v_1 +v_3) and 1101 cm^{-1} (v_1) [21,22]. The bands at 2342 and 2276 cm^{-1} were assigned to v_3 vibrations of $^{12}CO_2$ and $^{13}CO_2$, respectively. The 2037 cm^{-1} band is attributed to CO_3 in complex with Cl [13]. In $CH_2ClCOCl/O_2$, the bands at 2157, 2152 and 835 cm^{-1} due to CHCl=C=O were observed. Absorption bands due to CH_2Cl_2 were observed at 1268 and 750 cm^{-1}.

3.4 Reaction Mechanism

Fig. 6 shows the absorbance changes of the C=O stretching vibration band for the CHCl=C=O···HCl π complex and the CCl_2 antisymmetric stretching vibration band for CH_2Cl_2 observed in Ar, Kr and Xe. The CHCl=C=O···HCl complex showed the growth and decay profiles in Kr and Xe. Therefore, the approximate relative yield, $\Phi_{CHCl=C=O\cdots HCl/CH2Cl2}$, of the above mentioned absorption bands of CHCl=C=O···HCl and CH_2Cl_2 at an irradiation time of 100 min was compared using the IR intensities of 618 and 149 km mol^{-1}, respectively, calculated at the B3LYP/aug-cc-pV(T+d)Z level. The values of $\Phi_{CHCl=C=O\cdots HCl/CH2Cl2}$ were 18, 5.2 and 0.82 for the Ar, Kr and Xe matrices, respectively. The formation of CH_2Cl_2 was greatly enhanced in Xe probably due to the external heavy atom effect. This observation indicates that changing the matrix gas from Ar to Kr or Xe may open

the reaction paths in the triplet state, $CH_2ClCOCl$ (T_1) → CH_2Cl + COCl → CH_2Cl + CO + Cl → CH_2Cl_2 + CO and $CH_2ClCOCl$ (T_1) → CH_2ClCO + Cl → CH_2Cl_2 + CO.

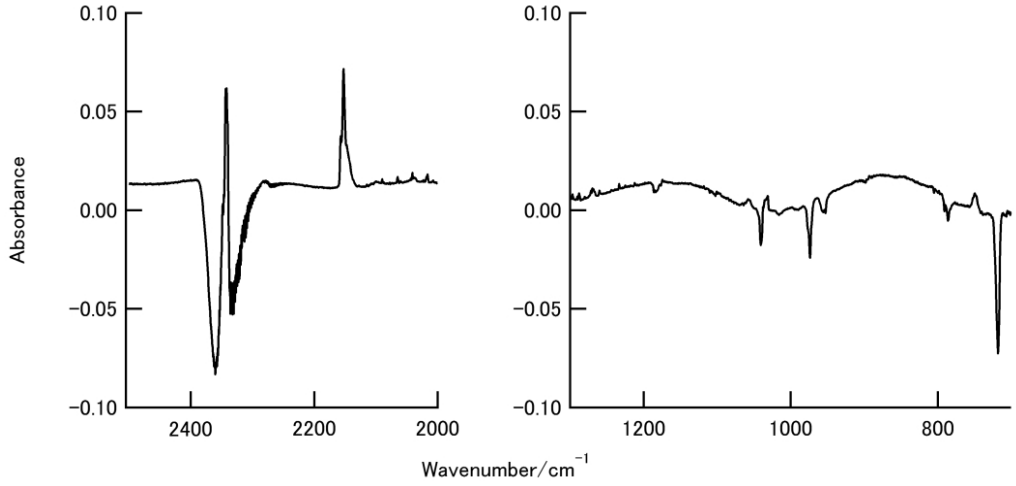

Fig. 5. Infrared difference spectrum upon λ > 253.7 nm irradiation of the matrix $CH_2ClCOCl/O_2$ = 1/1000 for 60 min

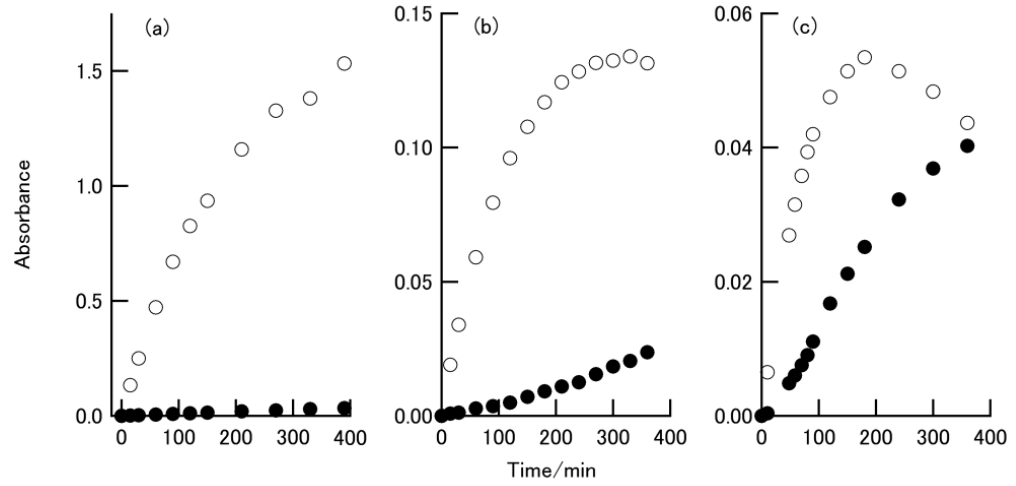

Fig. 6. Absorbance changes of CHCl=C=O and CH_2Cl_2 in (a) Ar, (b) Kr and (c) Xe

As shown in Fig. 5, the ketene species were produced in O_2, which was indicative of their formation through a concerted mechanism in the ground state. A small amount of CH_2Cl_2 was also observed in O_2. The energy diagram for the formation of the ketene species and CH_2Cl_2 in the ground state is shown in Fig. 7. The transition state TS3 for the formation of CH_2Cl_2 and CO lies in much higher compared with the TS2 for the formation of CHCl=C=O···HCl. This agreed with the observed predominant CHCl=C=O formation in Ar.

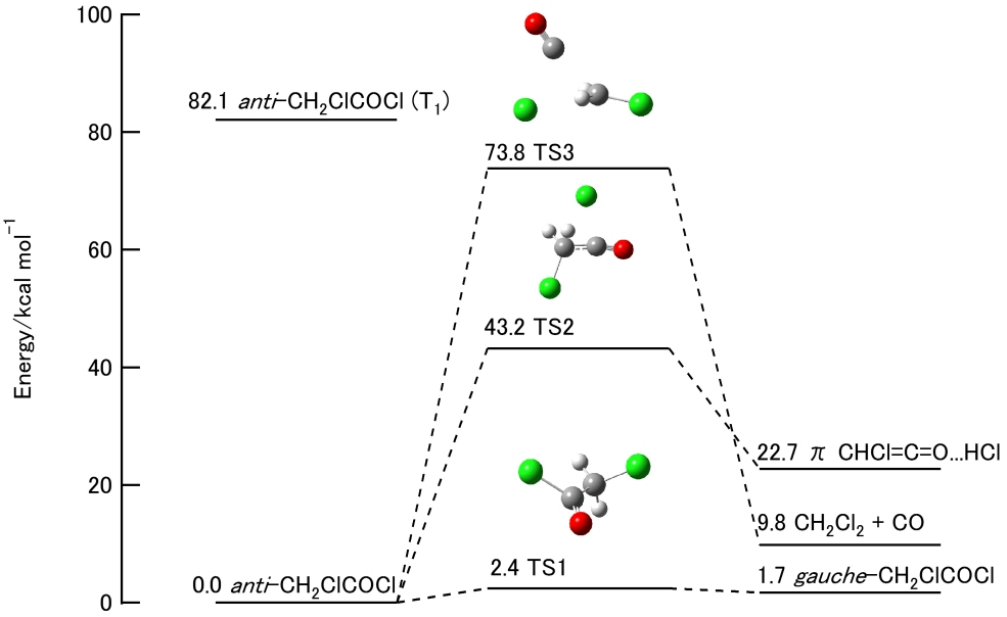

Fig. 7. Energy diagram for the reactions of $CH_2ClCOCl$ in the ground state calculated at the B3LYP/aug-cc-pV(T+d)Z level

4. CONCLUSION

UV light photolysis of $CH_2ClCOCl$ was investigated in cryogenic Ar, Kr, Xe and O_2 matrices. In $CH_2ClCOCl$/Ar, photoisomerization from *anti*- to *gauche*-$CH_2ClCOCl$ was observed at an early stage of the irradiation. In all matrices, CHCl=C=O, HCl, CH_2Cl_2 and CO were produced, with the relative yields depending on the used matrix gas The relative yield of CH_2Cl_2 formation was greatly enhanced in Xe because of the external heavy atom effect. The results show that in Ar, the reactions predominantly proceed through concerted mechanisms.

COMPETING INTERESTS

Authors have declared that no competing interests exist.

REFERENCES

1. Yamazaki-Nishida S, Cerveramarch S, Nagano KJ, Anderson MA, Hori K. Experimental and theoretical-study of the reaction-mechanism of the photoassisted catalytic degradation of trichloroethylene in the gas-phase. J Phys Chem. 1995;99(43):15814-15821.
2. Oki K, Tsuchida S, Nishikiori H, Tanaka N, Fujii T. Photocatalytic degradation of chlorinated ethenes. Int J Photoenergy. 2003;5(1):11-15.
3. Hasson AS, Smith IWM. Chlorine atom initiated oxidation of chlorinated ethenes: Results for 1, 1-dichloroethene ($H_2C=CCl_2$), 1, 2-dichloroethene (HClC=CClH), trichloroethene ($HClC=CCl_2$) and tetrachloroethene ($Cl_2C=CCl_2$). J Phys Chem A. 1999;103(13):2031-2043.

4. Wiltshire KS, Almond MJ, Mitchell PCH. Reactions of hydroxyl radicals with trichloroethene and tetrachloroethene in argon matrices at 12 K. Phys Chem Chem Phys. 2004;6(1):58-63.
5. Nakagawa I, Ichishima I, Kuratani K, Miyazawa T, Shimanouchi T, Mizushima S. Rotational isomers of chloroacetyl chloride, bromoacetyl chloride and bromoacetyl bromide. J Chem Phys. 1952;20(11):1720-1723.
6. Durig JR, Zhao W, Lewis DE, Little TS. Barriers to internal rotation, vibrational assignment, and ab initio calculations for chloroacetyl chloride. Chem Phys. 1988;128(2-3):353-365.
7. Little TS, Wang AY, Durig JR. Structural determinations of the haloacetyl halides by experimental and computational methods. J Mol Struct. 1990;217:221-238.
8. Davidovics G, Allouche A, Monnier M. Ab initio calculations and vibrational assignment of chloroacetyl chloride trapped in a low-temperature xenon matrix. J Mol Struct. 1991;243(1-2):1-12.
9. El-Bindary AA, Klaeboe P, Nielsen CJ. The conformational equilibria and vibrational-spectra, including infrared matrix-isolation spectra, of chloroacetyl chloride and chloroacetyl bromide. Acta Chemica Scandinavica. 1991;45(9):877-886.
10. Garcia MV, Raso MA, Lopez A. Infrared study of solvent influence on the rotational equilibrium in chloro and dichloroacetyl chloride. Anales De Quimica. 1992;88(5-6):534-541.
11. Allen GR, Russell DK. Laser pyrolysis studies of the thermal decomposition of chlorinated organic compounds. Part 1-Acyl chlorides. New J Chem. 2004;28(9):1107-1115.
12. Davidovics G, Monnier M, Allouche A. FT-IR spectral data and ab initio calculations for haloketenes. Chem Phys. 1991;150(3):395-403.
13. Tamezane T, Tanaka N, Nishikiori H, Fujii T. Matrix isolation and theoretical study on the photolysis of trichloroacetyl chloride. Chem Phys Lett. 2006;423(4-6):434-438.
14. Kogure N, Ono T, Suzuki E, Watari F. Photolysis of matrix-isolated acetyl-chloride and infrared-spectrum of the 1:1 molecular-complex of hydrogen-chloride with ketene in solid argon. J Mol Struct. 1993;296(1-2):1-4.
15. Rowland B, Hess WP. UV photochemistry of thin film and matrix-isolated acetyl chloride by polarized FTIR. J Phys Chem A. 1997;101(43):8049-8056.
16. Dellavedova CO, Rubio RE. Photolysis of matrix-isolated perfluoroacetyl chloride, $CF_3C(O)Cl$. J Mol Struct. 1994;321(3):279-281.
17. Becke AD. Density-functional thermochemistry .3. The role of exact exchange. J Chem Phys. 1993;98(7):5648-5652.
18. Lee C, Yang W, Parr RG. Development of the colic-salvetti correlation-energy formula into a functional of the electron density. Phys Rev B. 1988;37(2):785-789.
19. Frisch MJ, Trucks GW, Schlegel HB, Scuseria GE, Robb MA, Cheeseman JR, Scalmani G, Barone V, Mennucci B, Petersson GA, Nakatsuji H, Caricato M, Li X, Hratchian HP, Izmaylov AF, Bloino J, Zheng G, Sonnenberg JL, Hada M, Ehara M, Toyota K, Fukuda R, Hasegawa J, Ishida M, Nakajima T, Honda Y, Kitao O, Nakai H, Vreven TJA. Montgomery J, Peralta JE, Ogliaro F, Bearpark M, Heyd JJ, Brothers E, Kudin KN, Staroverov VN, Keith T, Kobayashi R, Normand J, Raghavachari K, Rendell A, Burant JC, Iyengar SS, Tomasi J, Cossi M, Rega N, Millam JM, Klene M, Knox JE, Cross JB, Bakken V, C. Adamo, Jaramillo J, Gomperts R, Stratmann RE, Yazyev O, Austin AJ, Cammi R, Pomelli C, Ochterski JW, Martin RL, Morokuma K, Zakrzewski VG, Voth GA, Salvador P, Dannenberg JJ, Dapprich S, Daniels AD, Farkas Ö, Foresman JB, Ortiz JV, Cioslowski J, Fox DJ. Gaussian 09, Revision D.01, Wallingford: Gaussian, Inc.; 2013.

20. Richter A, Meyer H, Kausche T, Muller T, Sporleder W, Schweig A. Electron attachment products of methylene chloride in solid argon: An experimental and quantum chemical IR spectroscopic study. Chem Phys. 1997;214(2-3):321-328.
21. Schriver-Mazzuoli L, Schriver A, Lugez C, Perrin A, Camy-Peyret C, Flaud JM. Vibrational spectra of the $^{16}O/^{17}O/^{18}O$ substituted ozone molecule isolated in matrices. Journal of Molecular Spectroscopy. 1996;176(1):85-94.
22. Schriver-Mazzuoli L, De Saxcé A, Lugez C, Camy-Peyret C, Schriver A. Ozone generation through photolysis of an oxygen matrix at 11 K: Fourier transform infrared spectroscopy identification of the $O\cdots O_3$ complex and isotopic studies. J Chem Phys. 1995;102(2):690-701.
23. Kunttu HM, Seetula JA. Photogeneration of ionic species in Ar, Kr and Xe matrices doped with HCl, HBr and HI. Chem Phys. 1994;189(2):273-292.
24. Carver TG, Andrews L. Matrix infrared spectrum and bonding in the dichloromethyl radical. J Chem Phys. 1969;50(10):4235-4244.
25. Sumathi R, Chandra AK. Quantum chemical study of hydrogen-bonded $CH_2=C=O\ldots HX$ and $CH_2=C=CH_2\ldots HX$ (X=Cl, F) complexes. Chem Phys Lett. 1997;271(4-6):287-295.

© 2014 Tanaka and Nakata; This is an Open Access article distributed under the terms of the Creative Commons Attribution License (http://creativecommons.org/licenses/by/3.0), which permits unrestricted use, distribution, and reproduction in any medium, provided the original work is properly cited.

Peer-review history:
The peer review history for this paper can be accessed here:
http://www.sciencedomain.org/review-history.php?iid=536&id=7&aid=5340